

The GCR intensity and the models of the global heliospheric current sheet

Mikhail Kalinin, Mikhail Krainev

Lebedev Physical Institute, Russian Academy of Sciences,
Leninsky Prospect, 53, Moscow, 119991, Russia

Abstract. The form of the global heliospheric current sheet and some modified tilted current sheet models are considered. The different forms of the scaling factor of the regular drift velocity and current sheet drift velocity and the response of the GCR intensity are discussed.

Keywords: Heliospheric current sheet, galactic cosmic rays

I. INTRODUCTION

According to the present-day notions the global heliospheric current sheet (HCS) plays an important role in the modulation of the galactic cosmic rays as it provides the very effective channel of their transportation. However, the HCS model usually used in cosmic ray studies, the tilted current sheet (TCS), is in our opinion oversimplified.

In Section I some modified tilted current sheet (MTCS) models are considered to bring the model closer to the observed HCS and to get the more physical current sheet with finite thickness and normal component of the magnetic field. In Section II we discuss the different forms of the scaling factor of the regular drift velocity and current sheet drift velocity corresponding to different HCS models and in some cases solve the 2D transport equation and compare the GCR response to the HCS models.

II. THE MODELS OF THE HELIOSPHERIC CURRENT SHEET

Like any physical object the heliospheric current sheet should have the finite thickness and some structure. However, if the Larmor radius is much less than this thickness the latter can be neglected when studying the transport of the particles. Then the magnetic field is $\vec{B} = \mathcal{F}\vec{B}_m$, where \vec{B}_m is the ‘‘monopolar’’ magnetic field and \mathcal{F} is a scalar function equal to ± 1 in the positive and negative sectors. Usually the HCS surface $\mathcal{F}(r, \vartheta, \varphi, t) = 0$ has rather complicated form, so it is natural to check if it can be described by simpler models.

Nevertheless, the current sheet without normal component of the magnetic field is unstable (see, e. g., [8]). So one should estimate the structure of the HCS and how it can influence the characteristics important for the GCR intensity. Here we discuss the unsteady state of the HCS as the cause of its finite thickness and \mathcal{B}_n , although the finite HCS structure can be in the steady state as well.

A. Infinitely thin HCS without \mathcal{B}_n

In a simple but rather effective Wilcox Solar Observatory (WSO) model of the HCS formation, its base, isoline $\mathcal{B}_r = 0$ at the source surface $r_{ss} = (2.5 \div 3.25)r_\odot$, is calculated for each Carrington rotation in potential approximation using the measured photospheric line-of-sight magnetic field \mathcal{B}_{l_s} with $\mathcal{B}_{\vartheta, \varphi} = 0$ at r_{ss} as outer boundary condition and two variants of the inner boundary conditions: fixing \mathcal{B}_{l_s} (classic) and \mathcal{B}_r (radial), see [3] and references therein. Both sets of the spherical harmonics coefficients are available at the WSO site, [11]. It is believed that HCS produced by transporting this line to the heliosphere by the solar wind is in reasonably good agreement with the observed crossings of the HCS. So here we consider this calculated HCSs as the ‘‘observed’’ ones which should be approximated by the simple HCS models to be used in cosmic ray studies.

Besides, in the same site one can find (in Tilt.html file) the minimum λ_{min}^{CS} and maximum λ_{max}^{CS} latitudes of the calculated HCS. In cosmic ray studies a tilted current sheet (TCS) model is usually used with the base of the HCS taken to be a great circle tilted to the equator by $\alpha^{CS} = (\lambda_{max}^{CS} - \lambda_{min}^{CS})/2$, [10],[2]. From the same data the latitude of the magnetic equator can be estimated, $\vartheta_{me}^{CS} = \pi/2 - (\lambda_{max}^{CS} + \lambda_{min}^{CS})/2$.

In the simplest model the colatitude of the HCS on the source surface $\vartheta^{CS} = \vartheta_{me}^{CS} - \arctan(\tan\alpha^{CS} \sin\varphi)$. However, this expression implies that the longitude of the ascending node φ^{CS} is zero and φ^{CS} corresponding to the real HCS should be fixed. Besides, the estimation of the amplitudes of the HCS and magnetic equator from the Tilt.html data is rather rough and the complex heliospheric magnetic field often has a four-sector (or, generally, $2k$ -sector) structure, which can hardly be described by the model of the great circle tilted at some angle. So we formed the following MTCS models:

$$\vartheta^{CS} = \vartheta_{me}^{CS} - \arctan(\tan\alpha^{CS} \sin(\varphi - \varphi^{CS})) \quad (1)$$

$$\vartheta^{CS} = \vartheta_{me}^{CS} - \arctan(\tan\alpha^{CS} \sin(\varphi - \varphi^{CS})) \quad (2)$$

$$\vartheta^{CS} = \vartheta_{me}^{CS} - \arctan(\tan\alpha^{CS} \sin(\varphi - \varphi^{CS})) \quad (3)$$

where the underlined parameters are the free parameters that should be fixed, while the not-underlined ones are taken from the Tilt-file. The MTCS model (1) has one free parameter φ^{CS} (we call it MTCS01 model), the model (2) has two free parameters $\vartheta_{me}^{CS}, \varphi^{CS}$ (MTCS02 model) and in MTCS04 model there are four free

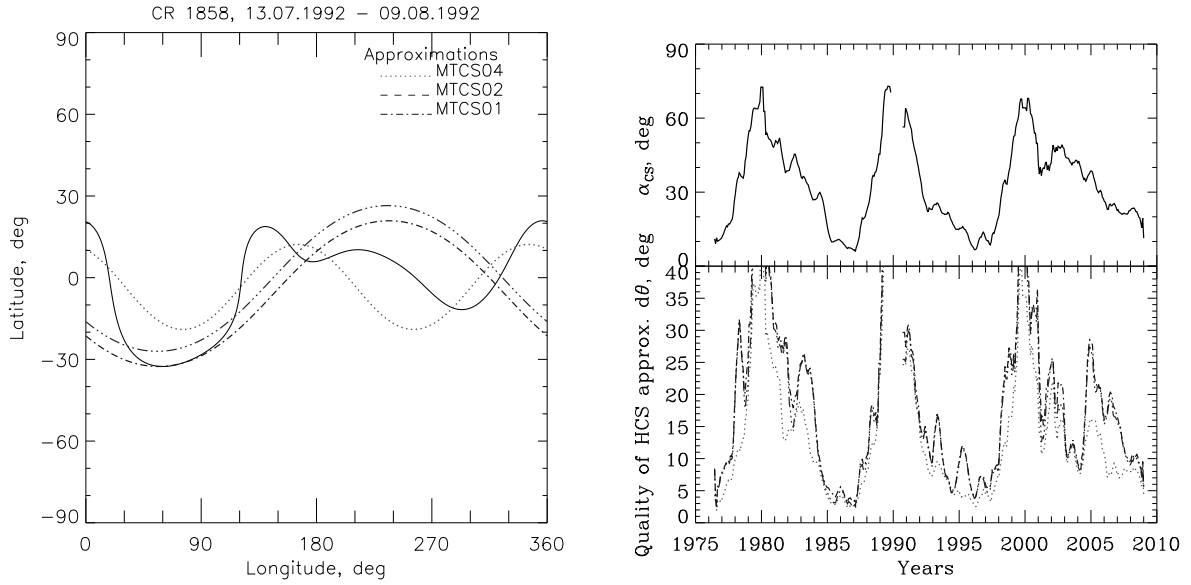


Fig. 1: The approximation of the "observed" HCS (radial inner boundary condition) using the modified current sheet models. The left panel: the approximation of HCS by the models (1-3) for typical CR1858. The right panels: the time behavior of the tilt (upper panel) and the quality of the HCS approximation for 1976-2009 (lower panel).

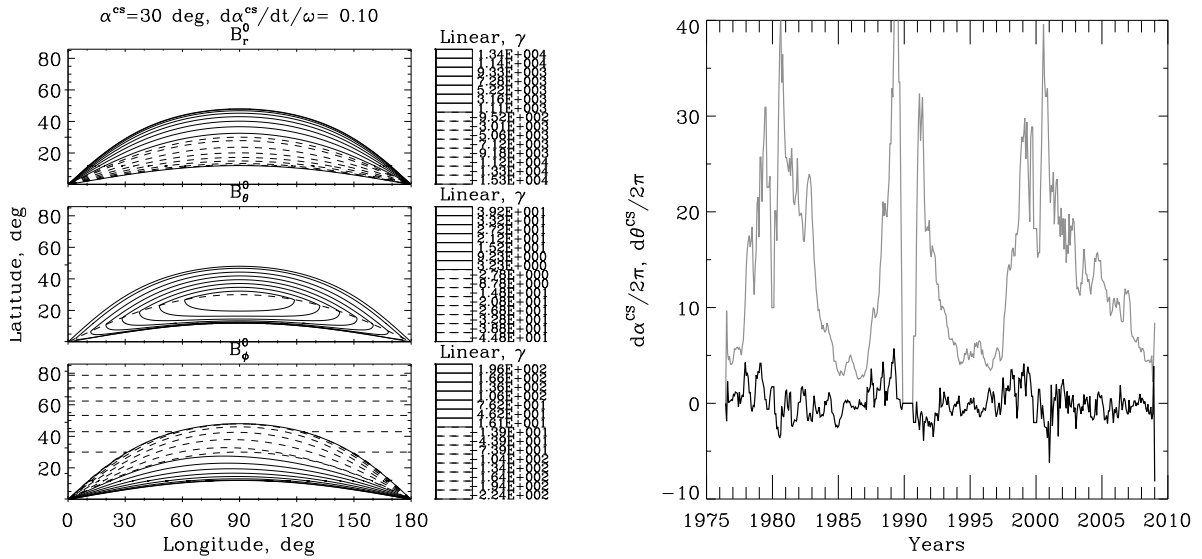


Fig. 2: The magnetic field on the source surface according to the MTCS11 model and the time behavior of the related HCS characteristics. The left panel: the $B_{r,\vartheta,\varphi}$ on the source surface according to (4-6) for the case illustrated (see text). The right panel: the time behavior of the changes in α^{CS} and the MRS difference in colatitude between the consequent HCSs for 1976-2009.

parameters $\vartheta_{me}^{CS}, \alpha^{CS}, k^{CS}, \varphi^{CS}$ without any data from the Tilt-file.

The HCSs were calculated for each Carrington rotation (for both variants) and approximated with the models (1-3) using the downhill simplex method, [9]. The quality of the approximation was estimated as mean root square difference in colatitude between the "observed" and approximated HCSs.

In Fig.1 the results of the approximation for HCS

(radial inner boundary condition; $r_{ss} = 3.25r_{\odot}$) are shown. One can see that even though the quality of the approximation is better for MTCS04 model than for MTCS01 and MTCS02, all the models are rather rough, so it is much preferable to use the "observed" HCSs for the cosmic ray studies.

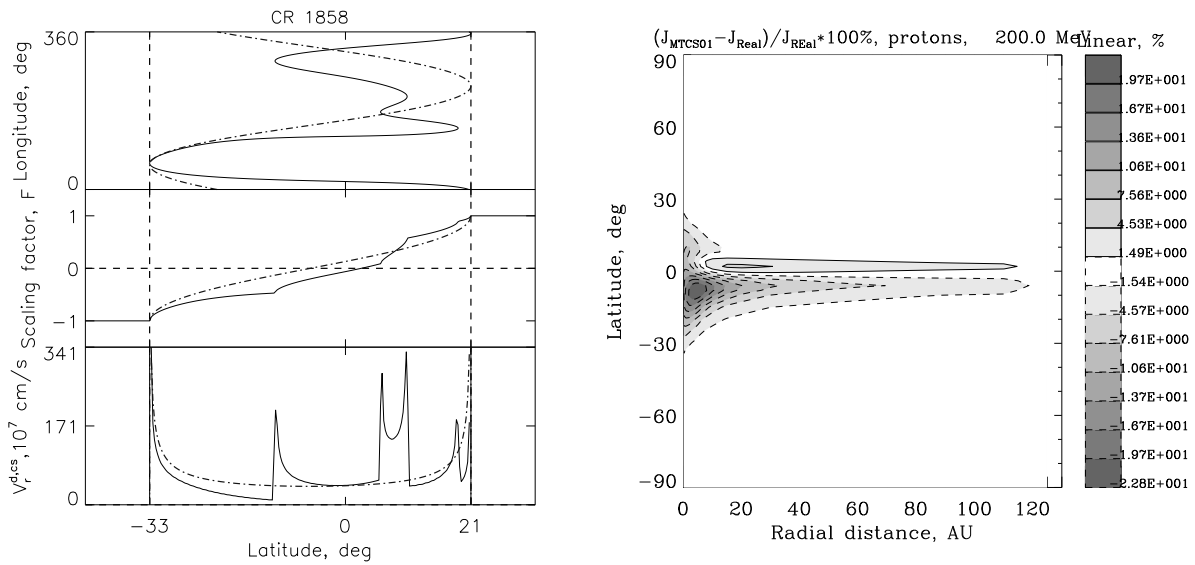


Fig. 3: The comparison of the HCS, drift characteristics and GCR intensity for the MTCS01 model and the "observed" HCS for CR1858. The left panels: the form of the CS (upper panel) and the averaged over the longitude the scaling factor of the regular drift velocity (middle) and the current sheet drift velocity. The solid and dot-dashed curves are for the real HCS and the MTCS01 model, respectively. The right panel: the relative difference between the GCR intensity for MTCS model and real HCS as a function of ϑ, φ .

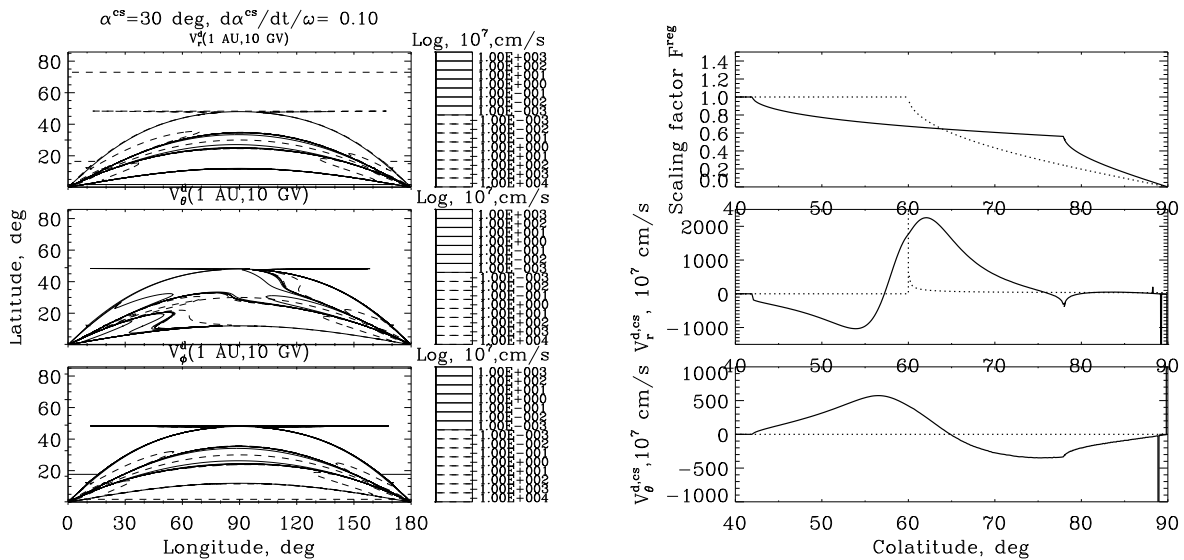


Fig. 4: The current sheet drift velocity and its averaged over the longitude characteristics according to the MTCS11 model. The left panels: the three components of the current sheet drift velocity at $r = 1 \text{ AU}, R = 10 \text{ GV}$. The right panels: the comparison of the averaged over the longitude scaling factor of the regular drift velocity (upper panel), the radial (middle) and latitudinal (lower) components of the current sheet drift velocity. The solid and dotted curves are for the MTCS11 and TCS models with the same α^{cs} , respectively.

B. HCS with finite thickness and B_n

As one can see from the left panel of Fig.1, the tilt of the HCS is changing during the solar cycle. It means that on the source surface \mathcal{B}_r is also changing near the $\mathcal{B}_r = 0$ line which results in $\mathcal{B}_{\vartheta}, \mathcal{B}_{\varphi}$ components (see, e. g., [1], [4]). We found $\vec{\mathcal{B}}(r, \vartheta, \varphi)$ averaged over the period

of Carrington rotation T for the TCS rotating around equatorial $\varphi = \varphi^{cs}$ line from $\alpha^{cs} - \delta\alpha^{cs}$ to $\alpha^{cs} + \delta\alpha^{cs}$ with the changing angular velocity $\dot{\alpha}^{cs}$ (and averaged angular velocity $\langle \dot{\alpha}^{cs} \rangle_T = 2\delta\alpha^{cs}/T$):

$$\mathcal{B}_r = -\mathcal{B}_0 \left(1 - \frac{2\tilde{t}}{T}\right) \quad (4)$$

$$\mathcal{B}_\vartheta = \frac{2\mathcal{B}_0 r_0}{\mathcal{V}^{sw}} \dot{\alpha}^{cs} \left(1 - \frac{\tilde{t}}{T}\right) \sin \varphi \quad (5)$$

$$\mathcal{B}_\varphi = \frac{2\mathcal{B}_0 r_0}{\mathcal{V}^{sw}} \dot{\alpha}^{cs} \left(1 - \frac{\tilde{t}}{T}\right) \cos \varphi \cos \vartheta - \frac{r_0 \omega \sin \vartheta}{\mathcal{V}^{sw}} \mathcal{B}_r \quad (6)$$

where $\mathcal{B}_0, \omega, \mathcal{V}^{sw}$ are the radial component of magnetic field on the source surface out of the CS, angular velocity of the Sun, and the constant solar wind velocity, respectively, and \tilde{t} is some function of $\alpha^{cs}, d\alpha^{cs}/dt, \vartheta, \varphi$ equal to the time when the CS reaches the point $\{\vartheta, \varphi\}$ during its rotation. For details of this model (we call it MTCS11) see [6]

In the left panel of Fig. 2 we illustrated the structure of magnetic field in the rather wide CS ($\alpha^{cs} = 30, \langle \dot{\alpha}^{cs} \rangle_T / \omega = 0.1$) and the case when the CS rotates with constant acceleration during the half of the period and then rotates with constant deceleration to the end. It can be seen that in this MTCS11 model there are all three components of the magnetic field. But even in this case of the wide HCS the ratio of the normal component of the magnetic field to the radial component out of the CS is very small, $\mathcal{B}_\vartheta / \mathcal{B}_0 \leq 10^{-3}$. As one can see from the right panel of Fig. 2 the real $\langle \dot{\alpha}^{cs} \rangle_T / \omega$ are much smaller than 0.1, so the maximum and average \mathcal{B}_n are also much lower than those shown in the left panel of Fig.2.

However, the mean root square difference in colatitude between the consequent HCSs also shown in the right panel of Fig. 2 is much greater than $\langle \dot{\alpha}^{cs} \rangle_T$, and for this case the average \mathcal{B}_n can be comparable with those in the left panel of Fig. 2. So the question if the thickness and normal component of the magnetic field due to the unsteady nature of the HCS can play any role is still open. Besides, the finite structure of the HCS can arise in the steady state as well (see [8]).

III. THE GCR INTENSITY AND HCS MODELS

To study the influence on the GCR intensity of the form of the infinitely thin HCS and its models, the zero approximation (see [5]) the equation for the 2D omnidirectional GCR distribution function was solved. In this case the HCS-effect on the averaged drift velocity can be described using the scaling factor F of the regular magnetic drift velocity and the unit vector \mathbf{n}^{cs} normal to the HCS surface. In the left panel of Fig. 3 the HCS form, the scaling factor and averaged current sheet drift velocity are compared for the MTCS01 model and the real HCS. To our minds it is important that 1) for the real HCS there are localized peaks in the current drift velocity latitude profile absent in the MTCS01 model and 2) for the real HCS the latitude of the magnetic equator (where $F = 0$, i. e., the regular drift velocity

changes sign) is quite different from that used in MTCS01 model (from the Tilt-file).

The relative difference in the distribution of the GCR intensity in the $r - \vartheta$ -plane is calculated with the drift velocity corresponding to the MTCS01 model and real HCS (CR1858, $A > 0$) and shown in the left panel of Fig. 3 for the medium energy protons. It can be seen that the above two factors (the change of the magnetic equator and peaks in the current sheet velocity) result in rather localized difference in the intensity for small heliocentric distances. It can be checked using near-the-Earth and Ulysses spacecraft.

For the MTCS11 model of the HCS with finite thickness and normal magnetic field component in the left panel of Fig. 4 all three components of the magnetic drift velocity are shown calculated using the distribution of the magnetic field shown in Fig. 2 (left panel) for $r = 10$ AU and $R = 10$ GV. It can be seen that there is a complicated structure of the wide HCS in this MTCS11 model, especially for \mathcal{B}_ϑ -component. In the right panel of the same figure the colatitude profiles of the averaged over the longitude characteristics of the magnetic drift velocity are compared for this MTCS11 model and for TCS model with the same α^{cs} . One can easily see the structure in the MTCS11 current sheet velocity both in the radial and latitudinal components. Note that in TCS model $\mathcal{B}_\vartheta = 0$.

As to the effects of the HCS model with finite thickness and normal magnetic field component, we are going to study them after we constructed the more reliable and close to nature model.

ACKNOWLEDGMENT

The authors acknowledge the Russian Fond for Basic Research (RFBR; grant 08-02-00418).

REFERENCES

- [1] Alekseev I.I., Veselovsky I.S., Kropotkin A.P., *Geomagnetism and Aeronomy*, **32**, N1, p.5-9, 1982
- [2] Jokipii J.R., Thomas B., *Ap. J.*, **243**, p.1115-1122, 1981
- [3] Hoeksema J. T., Ph.D. Thesis, Stanford university, USA, 1984
- [4] Kalinin M.S., Krainev M.B., Makhmutov V.S., *Proc. 23rd ICRC, Calgary, Canada*, **3**, p.543-546, 1993
- [5] Krainev M.B., Kalinin M.S., On the exact 2D transport equation for the GCR intensity averaged over the heliolongitude, this conference, 2009
- [6] Kalinin M.S., Krainev M.B., SW-12 conference, Saint-Malo, France, 2009 (to be published)
- [7] M.S. Kalinin , PhD Thesis, Lebedev Physical Institute, 146p., in Russian, (2000)
- [8] Podgorny I.M., Podgorny A.I., *Int. Journ. Geomagnetism and Aeronomy*, **6**,G11005, doi:10.1029/2004GI000077, 2005
- [9] Press W.H. et al., *Numerical Recipes in C: The Art of Scientific Computing*, second edition, 528pp., Cambridge University Press, 1992
- [10] Schultz M., *Astrophys. Space Sci.*, **24**, p.371, 1973
- [11] <http://sun.stanford.edu/wso/wso.html>